

M. DOŚPIAŁ*[‡], M. NABIALEK*, K. BŁOCH*

INFLUENCE OF COOLING RATE ON PHASE COMPOSITION AND MAGNETIC PROPERTIES OF $\text{Sm}_{12.5}\text{Co}_{66.5}\text{Fe}_8\text{Cu}_{11}\text{Si}_2$ ALLOY IN THE FORM OF RIBBON IN AS-QUENCHED STATE

WPLYW SZYBKOŚCI CHŁODZENIA NA SKŁAD FAZOWY I WŁASNOŚCI MAGNETYCZNE STOPU $\text{Sm}_{12.5}\text{Co}_{66.5}\text{Fe}_8\text{Cu}_{11}\text{Si}_2$ W STANIE PO ZESTALENIU

The fabrication method and magnetic properties of $\text{Sm}_{12.5}\text{Co}_{66.5}\text{Fe}_8\text{Cu}_{11}\text{Si}_2$ alloy are presented in this article. The samples were produced by rapid quenching of the liquid alloy onto a rotating, copper wheel (the so-called 'melt-spinning' method) and they had a thin ribbon shape. The microstructure of the samples was investigated by measurements of diffraction patterns for powdered samples, in order to obtain data from the entire volume of the sample. It was found, that samples were composed of different amounts of $\text{Sm}_2\text{Co}_{17}$, SmCo_5 and SmCo_7 phases, depending on the linear velocity of the copper wheel used during the fabrication process. The magnetic measurements were performed using a vibrating sample magnetometer (LakeShore VSM) working with an external magnetic field of up to 2 T. It was found that the obtained ribbons displayed relatively good hard magnetic properties, such as remanence $\mu_0 M_R$, and high resistance to demagnetization fields $J_H C$.

Keywords: Rare earth metals and alloys, Permanent magnets, Magnetization reversal mechanisms

W pracy badano wpływ warunków wytwarzania na własności magnetyczne i skład fazowy stopu $\text{Sm}_{12.5}\text{Co}_{66.5}\text{Fe}_8\text{Cu}_{11}\text{Si}_2$ w stanie po zestaleniu. Próbki stopu zostały otrzymane przy użyciu metody szybkiego chłodzenia na miedzianym wirującym bębnie (ang. melt-spinning) i miały postać cienkich taśm. Badania struktury zostały wykonane przy użyciu dyfraktometru rentgenowskiego. W celu otrzymania danych z całej objętości próbki badania składu fazowego zostały przeprowadzone dla sproszkowanych próbek. Dla otrzymanych dyfraktogramów przeprowadzono analizę jakościową i ilościową (Rietvelde) składu fazowego. Na podstawie otrzymanych wyników stwierdzono, że próbki składały się z różnych zawartości faz $\text{Sm}_2\text{Co}_{17}$, SmCo_5 i SmCo_7 . Nawet niewielkie zmiany w szybkości chłodzenia skutkują znacznymi różnicami w składzie fazowym stopu. Własności magnetyczne próbek zostały wyznaczone przy użyciu magnetometru wibracyjnego (LakeShore VSM), przy zastosowaniu zewnętrznego pola magnetycznego o wartości 2T. Różna zawartość faz oraz rozmiary ziaren w otrzymanych próbkach powodowały znaczne różnice w wartościach parametrów magnetycznych.

1. Introduction

At present, the papers related with SmCo based permanent magnets are divided into two main themes, i.e. the manufacture of magnets with high coercivity, unique cluster structure and strong magnetocrystalline anisotropy, [1], and magnets with much poorer magnetic properties but which feature high temperature stability of up to 400°C. For the latter type, the materials are based on $\text{Sm}(\text{Co}, \text{M})_7$ compound, where M represents the type of alloying additions, that enforce formation of TbCu_7 unique, metastable structure [2-4]. Investigations performed by other scientists [5, 6] have shown, that alloys with SmCo_7 structure, besides the high Curie temperature and ($T_C \sim 800^\circ\text{C}$), possess lower or even abnormal coercivity temperature coefficients ($b = -0.10$ to $-0.16\% \text{ } ^\circ\text{C}^{-1}$).

Since the metastable SmCo_7 phase cannot exist in isolation, the addition of a third alloying component, M, such as: Si, Cu, Ga, Nb, or Hf is used. These components facilitate

the formation and stabilisation of the SmCo_7 phase, [7-10]. Moreover, some of the magnetic properties of the alloys can be improved. If the electronegativity of added component(s) M is smaller than for Co, atoms of alloying additives prefer certain locations in the lattice (2e instead of 3g). However, if the amount of M is too great ($x > 3$) its atoms will prefer location 2c, [11, 12]. If alloying additive atoms take locations 2e and 3g in the SmCo_7 lattice, there is an increase in magnetocrystalline anisotropy and an improvement in magnetic properties, whereas atoms taking location 2c cause a decrease in magnetocrystalline anisotropy and a worsening of magnetic properties. In Fig. 1, the unit cell of SmCo_7 , together with the locations of atoms, are shown.

In this paper, the influence of cooling rate on the phase composition and magnetic properties of the $\text{Sm}_{12.5}\text{Co}_{66.5}\text{Fe}_8\text{Cu}_{11}\text{Si}_2$ alloy in the as-quenched state are investigated.

* INSTITUTE OF PHYSICS, CZESTOCHOWA UNIVERSITY OF TECHNOLOGY, 19 ARMII KRAJOWEJ AVE., 42-200 CZĘSTOCHOWA, POLAND

[‡] Corresponding author: mdospial@wp.pl

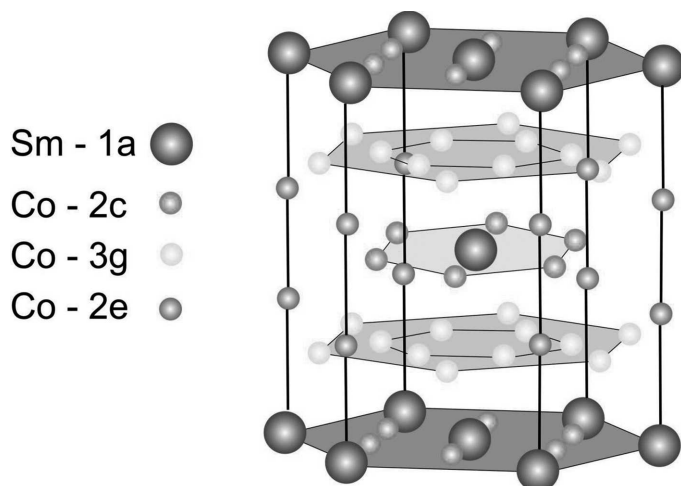


Fig. 1. The unit cell of SmCo_7 , [13]

2. Materials and Methods

2.1. Materials

Crystalline ingots of $\text{Sm}_{12.5}\text{Co}_{66.5}\text{Fe}_8\text{Cu}_{11}\text{Si}_2$ alloy were prepared, using a plasma arc, from components of the following purities: Fe – 99.98, Co – 99.99, Sm – 99.9, Cu – 99.99, Si – 99.99, Fe – 99.98. The ingots were re-melted several times in order to ensure homogeneity of the resulting alloy. Due the presence in the alloy of rare earth metal components, which are prone to oxidation, the whole process was performed, under a protective argon atmosphere. In addition, pure Ti was used as a ‘getter’.

In the next step, the prepared ingots were crushed into small pieces, sealed in quartz capillaries and mounted onto a melt spinner. Based on previous research, the production process parameters were chosen, including: pressure of the work chamber (0.4 Atm.), range of linear velocity of the copper wheel (18, 20 and 22 m/s), diameter of capillary opening (0.5 mm) and pressure of injecting gas, [5-10]. The crushed ingots were induction melted and injected onto the rotating copper wheel. The obtained samples were in the shape of ribbons, with thickness of 40 μm . The whole process was carried out under an inert atmosphere.

2.2. Methods

The X-ray diffraction investigations were performed by means of a Bruker X-ray diffractometer, equipped with a semiconductor counter. The X-ray diffraction patterns were obtained using a copper lamp with $K_{\alpha} = 1.54056 \text{ \AA}$. The samples were scanned in 2θ range, from 30° to 120° with increments of 0.02° and exposure time of 3 s per step.

On the basis of the obtained X-ray patterns, using the Rietveld method, the qualitative and quantitative analyses of the phase composition were performed. For qualitative analysis, ‘DIFFRAC.EVA’ software, equipped with PDF1 base, was used. Quantitative analysis was performed using ‘DifragPower’ software. The average grain size was calculated on the basis of analysis of the most intensive peaks in the X-ray diffraction patterns, using the Bragg equation, [14]:

$$\Delta^{hkl}(2\theta) \cdot \cos(\theta_B^{hkl}) = \frac{K \cdot \lambda}{D} + 2 \frac{\Delta d}{d} \cdot \sin(\theta_B^{hkl}) \quad (1)$$

where: D – grain size, K – shape coefficient (assumed value of 0.89), α – characteristic wavelength, Δ^{hkl} – peak half-width, given in radians, $\Delta d/d$ – the relative coefficient of deformation, θ_B^{hkl} – Bragg angle.

Samples used for the measurement of magnetic properties were in the form of ribbons with 0.5 mm length and 0.2 mm width. In order to perform the magnetic measurements, all samples were demagnetized using an alternating magnetic field. All alloys in the as-quenched state had vestigial spontaneous magnetization, as a result of magnetocrystalline anisotropy. These measurements were performed using a LakeShore magnetometer with a vibrating sample (VSM) in magnetic fields of up to 2 T. The demagnetization factor, resulting from magnetostatic field related with sample shape, was not taken into account.

All measurements were performed at room temperature.

3. Results and discussion

In Figs. 2a-4a the diffraction patterns for the samples are shown; comparison with existing databases has revealed that these ribbon samples feature three different crystalline phases in differing quantities. The three phases are: $\text{Sm}_2\text{Co}_{17}$, SmCo_5 , and SmCo_7 .

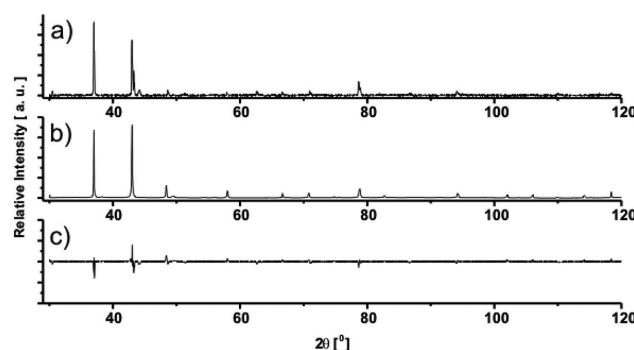


Fig. 2. X-ray diffraction patterns obtained for $\text{Sm}_{12.5}\text{Co}_{66.5}\text{Fe}_8\text{Cu}_{11}\text{Si}_2$ alloy, obtained using a wheel linear velocity of 18 m/s: a) measured, b) calculated from the Rietveld analysis, c) difference between measured and calculated results

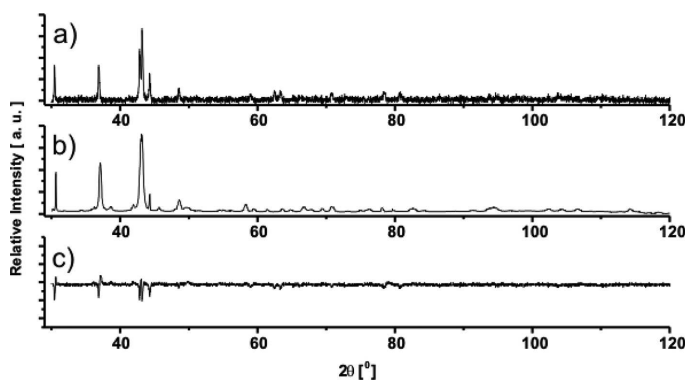


Fig. 3. X-ray diffraction patterns obtained for $\text{Sm}_{12.5}\text{Co}_{66.5}\text{Fe}_8\text{Cu}_{11}\text{Si}_2$ alloy, obtained using a wheel linear velocity of 20 m/s: a) measured, b) calculated from the Rietveld analysis, c) difference between measured and calculated results

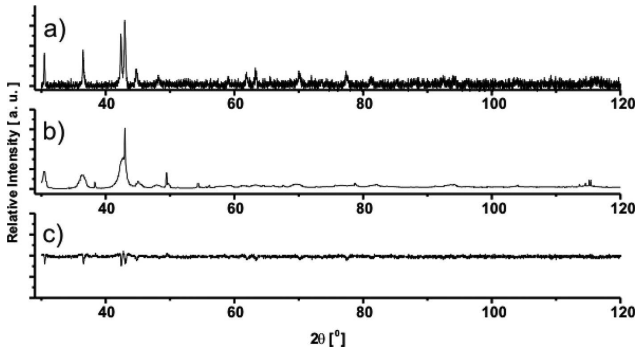


Fig. 4. X-ray diffraction patterns obtained for $Sm_{12.5}Co_{66.5}Fe_8Cu_{11}Si_2$ alloy, obtained using a wheel linear velocity of 22 m/s: a) measured, b) calculated from the Rietveld analysis, c) difference between measured and calculated results

In Figs. 2b-4b the patterns obtained from using the Rietveld analysis are shown. These patterns were used for two quantitative analyses of phase composition. The differences between experimental and simulated results (shown in Figs. 2c-4c) were mainly related with peak intensity and use of the copper lamp as a source of X-rays. It was found, that the sample prepared with the lowest linear velocity of the copper wheel (18 m/s) was composed from $SmCo_5$ and Sm_2Co_{17} phases.

From the comparison of experimental and Rietveld method results, it was found that the best fit was achieved for phase content of $SmCo_5$ and Sm_2Co_{17} equal to 92% and 8%, respectively. The average grain sizes, calculated from Equation 1, were equal to 220 nm for the Sm_2Co_{17} phase and 250 nm for the $SmCo_5$ phase. The sample obtained with a linear velocity of 20 m/s was found to consist of similar quantities of $SmCo_5$, Sm_2Co_{17} and $SmCo_7$ phases. The average grain sizes were found to be significantly smaller for samples prepared with lower cooling rates, and were equal to 120 nm, 150 nm and 100 nm, respectively for the $SmCo_5$, Sm_2Co_{17} and $SmCo_7$ phases. Sample number 3, obtained at the highest linear velocity of the copper wheel, had the highest value of $SmCo_7$ phase in the sample volume and the smallest grain sizes, equal to 75 nm and 80 nm for the Sm_2Co_{17} and $SmCo_7$, respectively.

The qualitative data, obtained using the Rietveld analysis, are shown in Fig. 5.

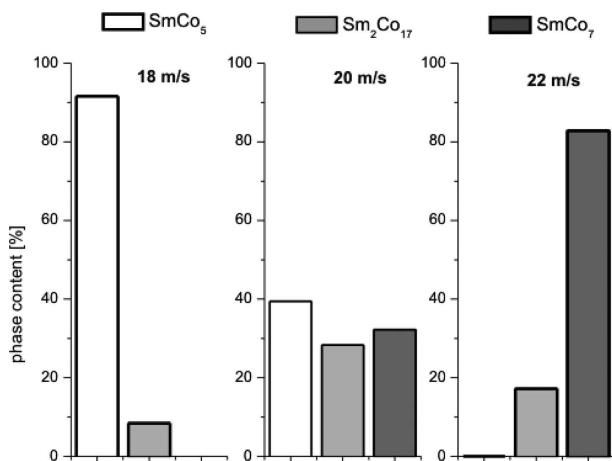


Fig. 5. The qualitative phase content in the volume of $Sm_{12.5}Co_{66.5}Fe_8Cu_{11}Si_2$ alloy, calculated from the Rietveld analysis

In Fig. 6 the magnetic hysteresis loops, measured in the magnetic field of up to 2 T, are shown.

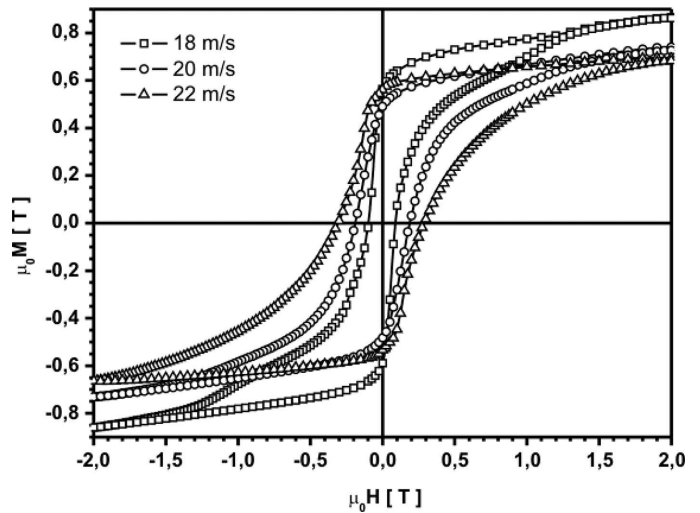


Fig. 6. Magnetic hysteresis loops, measured in the external magnetic field of up to 2 T

From the magnetic hysteresis loops, the magnetic parameters (i.e.: remanence μ_0M_R , coercivity JH_C , and saturation of magnetization μ_0M_S) were calculated and gathered in Table 1.

TABLE 1

Values of magnetic parameters obtained from hysteresis loop measurements: remanence (μ_0M_R), coercivity (JH_C), and saturation of magnetization (μ_0M_S)

Linear velocity of the wheel [m/s]	μ_0M_S [T]	μ_0M_R [T]	JH_C [kG]
18	0.88	0.57	1.0
20	0.74	0.49	1.9
22	0.70	0.56	3.1

The dependences of magnetic parameters on cooling rate are shown in Fig. 7. The sample cooled with the lowest speed yielded the highest saturation of magnetization; this result was unexpected, especially as the content of $SmCo_5$ phase in the sample volume is high and this phase has the lowest saturation of magnetization, compared with the other two phases. The values of this parameter for the two of remaining samples were lower and comparable with results obtained by other researchers for alloys with similar atomic compositions, [16, 17, 18]. The values of coercivity of the obtained magnets were in the range from 1 to 4 kG. Coercivity was found to increase with increasing cooling rate; this is believed to be connected with the refinement of the crystalline structure, which influences the creation of pinning sites. All of the investigated samples showed high remanence.

In order to find a better link between magnetic parameters and microstructure, the ratio of remanence, μ_0M_R (under a magnetic field equal to 2 T) to saturation of magnetization μ_0M_S (extrapolating to infinity) was found. The value of this ratio, for permanent magnets, should not exceed 0.50, unless the magnet is anisotropic or if exchange interactions exist between the grains, [15]. For the investigated samples, this ratio was found to be equal to 0.50, 0.55 and 0.75, for the samples

cooled with linear wheel velocity: 18, 20 and 22 m/s, respectively. For the sample with the medium cooling speed, the value of the ratio only slightly exceeded the required limit of 0.5, (being 0.55). The value of this ratio is within the expected range, given that the grain size is still relatively large (about 120 nm), and subsequently a small amount of SmCo₇ phase is in evidence (32%), and this phase is characterized, by a high value of magnetocrystalline anisotropy. Amongst the investigated samples, the best value of this ratio was given by the sample obtained with the highest linear velocity of the copper wheel. The high value of this ratio is influenced by the fine grain structure and high content of the strongly anisotropic SmCo₇ phase.

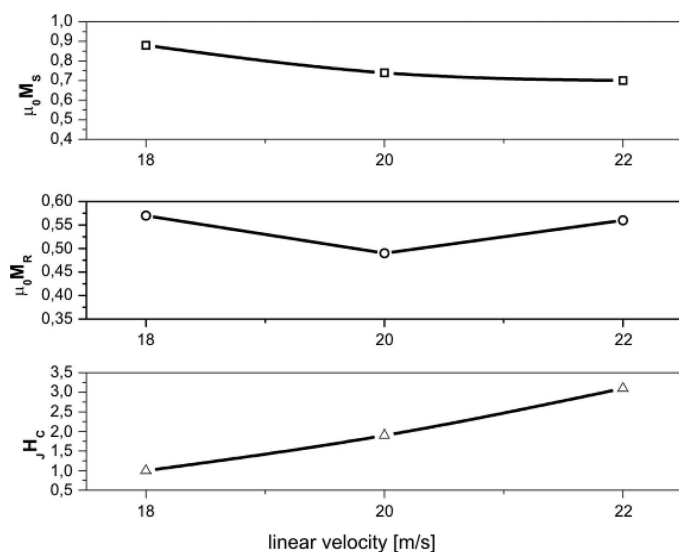


Fig. 7. Dependence of magnetic properties on the wheel velocity, for the investigated samples, obtained from magnetic hysteresis loop measurements

4. Conclusions

The carefully selected production process parameters and composition of the alloys facilitated the production of ribbons with TbCu₇-type structure.

The structure of the sample, obtained using the lowest linear wheel velocity, consisted mainly of the stable SmCo₅ phase. The highest content of the SmCo₇ phase, i.e. approximately 83%, was obtained for samples produced with the highest cooling rate. An increase in the cooling rate was connected with an increase in the content of the SmCo₇ phase in the sample volume.

The best hard magnetic properties were exhibited by the sample with the highest SmCo₇ phase content. The high value of the remanence to saturation of magnetization ratio (0.75) was influenced by the small grain size (approximately 80 nm) and strong magnetocrystalline anisotropy of the SmCo₇ phase. The high value of coercivity (for this type of magnet) is attributed to the refinement of the grain structure.

Acknowledgements

This work was financed by NCN, with the project number N N507 234940.

REFERENCES

- [1] A. Yan, A. Bollero, O. Gutfleisch, K.-H. Müller, L. Schultz, Melt-spun precipitation hardened Sm(Co, Fe, Cu, Zr)_z magnets, *Mat Sci Eng A* **375-377**, 1169-1172 (2004).
- [2] W. Tang, Y. Zhang, G.C. Hadjipanayis, *J Appl Phys* **91**, 7896 (2002).
- [3] D.T. Zhang, M. Yue, J.X. Zhang, L.J. Pan, *IEEE Trans Magn* **43**, 3494-6 (2007).
- [4] J. Zhou, I.A. Al-Omari, J.P. Liu, D.J. Sellmyer, *J Appl Phys* **87**, 5299 (2000).
- [5] H.W. Chang, S.T. Huang, C.W. Chang, C.H. Chiu et al., *J Appl Phys* **101**, 09K 508-3 (2007).
- [6] C.B. Jiang, M. Venkatesan, K. Gallagher, J.M.D. Coey, *J Magn Mater* 236-49 (2001).
- [7] H.W. Chang, S.T. Huang, C.W. Chang et al., *J Alloys and Compd* **455**, 506-509 (2008).
- [8] Y. Li, J. Shen, Y. Chen, *Solid State Sci* **12**, 33-38 (2010).
- [9] S.S. Makridis, I. Panagiotopoulos, I. Tsiaoussis et al., *J Magn Mater* **320**, 2322-2329 (2008).
- [10] M. Dospial, M. Nabialek, M. Szota, D. Plusa, *J Alloys and Compd* **509S**, S404-S407 (2011).
- [11] J. Luo, J.K. Liang, Y.Q. Guo, Q.L. Liu et al., *Intermetallics* **13**, 710 (2005).
- [12] Y.Q. Guo, W. Li, J. Luo, W.C. Feng, J.K. Liang, *J Magn Mater* **303**, e367 (2006).
- [13] M.J. Dospial, M.G. Nabialek, M. Szota, T. Mydlarz, K. Ożga, S. Lesz., *J. Alloys Compd.* **536**, S324-S328 (2012).
- [14] G.K. Willampson, W.H. Hall, *Acta Metall.* **1**, 22 (1953).
- [15] E.P. Wohlfarth, *J. Appl. Phys.* **29**, 595 (1958).
- [16] H. Wei, Z. Lingmin, Z. Yinghong, W. Ziqin, *J Alloys and Compd* **298**, 173-176 (2000).
- [17] Z.X. Zhang et al., *Scripta Materialia* **62**, 594-597 (2010).
- [18] M. Dośpiał, M. Nabiałek, M. Szota, Ł. Michta, P. Wiczorek, K. Błoch, P. Pietrusiewicz, K. Ożga, J. Michalczyk, *Optica Applicata XLIII*, 195-200 (2013).